J|A|C|S
ARTICLES
Published on Web 02/19/2004

Hydrogen Bond Geometries from Electron Paramagnetic Resonance and Electron−Nuclear Double Resonance Parameters: Density Functional Study of Quinone Radical Anion−Solvent Interactions

Sebastian Sinnecker, Eduard Reijerse, Frank Neese,* and Wolfgang Lubitz*

Contribution from the Max-Planck-Institut für Bioanorganische Chemie, Stiftstrasse 34-36, D-45470 Mülheim an der Ruhr, Germany

Received October 23, 2003; E-mail: Lubitz@mpi-muelheim.mpg.de; Neese@mpi-muelheim.mpg.de

Abstract: Density functional theory was used to study the impact of hydrogen bonding on the *p*-benzosemiquinone radical anion $BQ^{\bullet-}$ in coordination with water or alcohol molecules. After complete geometry optimizations, ^{1}H, ^{13}C, and ^{17}O hyperfine as well as ^{2}H nuclear quadrupole coupling constants and the **g**-tensor were computed. The suitability of different model systems with one, two, four, and 20 water molecules was tested; best agreement between theory and experiment could be obtained for the largest model system. Q-band pulse ^{2}H electron−nuclear double resonance (ENDOR) experiments were performed on $BQ^{\bullet-}$ in D_2O. They compare very well with the spectra simulated by use of the theoretical values from density functional theory. For $BQ^{\bullet-}$ in coordination with four water or alcohol molecules, rather similar hydrogen-bond lengths between 1.75 and 1.78 Å were calculated. Thus, the computed electron paramagnetic resonance (EPR) parameters are hardly distinguishable for the different solvents, in agreement with experimental findings. Furthermore, the distance dependence of the EPR parameters on the hydrogen-bond length was studied. The nuclear quadrupole and the dipolar hyperfine coupling constants of the bridging hydrogens show the expected $1/R^{3}_{O\cdots H}$ dependencies on the H-bond length $R_{O\cdots H}$. A $1/R^{2}_{O\cdots H}$ correlation was obtained for the **g**-tensor. It is shown that the point-dipole model is suitable for the estimation of hydrogen-bond lengths from anisotropic hyperfine coupling constants of the bridging ^{1}H nuclei for H-bond lengths larger than approximately 1.7 Å. Furthermore, the estimation of H-bond lengths from ^{2}H nuclear quadrupole coupling constants of bridging deuterium nuclei by empirical relations is discussed.

1. Introduction

Hydrogen bonding is considered to be the most important noncovalent interaction between molecules. It plays a vital role for the structure and function of many systems of chemical and biological relevance.[1−6] Quinones are prominent examples for which hydrogen bonding has been frequently reported. In biological systems they are met in many redox proteins, e.g., in the mitochondrial respiratory chain, in the reaction centers of bacterial and plant photosynthesis, and in many other systems.[7−11] Since hydrogen bonding affects the physical properties and thus the function of quinones, there has been considerable interest in elucidating the structural characteristics of these interactions in solution. As suitable methods, electronic absorption spectroscopy, fluorescence spectroscopy, vibrational spectroscopy, nuclear magnetic resonance, and nuclear quadrupole resonance methods have been used.[1,2,5] Furthermore, hydrogen bonding to quinone radicals and radical ions, which are frequent intermediates in quinone-mediated redox processes, can be studied in vitro and in vivo by electron spin resonance methods such as electron paramagnetic resonance (EPR) and electron−nuclear double resonance (ENDOR) spectroscopy.[12,13] These techniques provide insight into the electronic structure of paramagnetic species by means of **g**-tensors, hyperfine coupling constants (HFCC), and nuclear quadrupole coupling constants (NQCC). The **g**-tensor describes the interaction of the electron spin of the radical with the effective magnetic field. Furthermore, each magnetic nucleus *i* of the molecule interacts with the spin of the unpaired electron, which is described by the hyperfine tensor $\mathbf{A}_i$. Additionally, for all nuclei with spin

(1) Jeffrey, G. A. *An Introduction to Hydrogen Bonding*; Oxford University Press: New York, 1997.
(2) Vinogradov, S. N.; Linnell, R. H. *Hydrogen Bonding*; Van Nostrand Reinhold Company: New York, 1971.
(3) Scheiner, S. *Hydrogen Bonding. A Theoretical Perspective*; Oxford University Press: Oxford, U.K., 1997.
(4) Desiraju, G. R.; Steiner, T. *The Weak Hydrogen Bond in Structural Chemistry and Biology*; Oxford University Press: Oxford, U.K., 1999.
(5) Steiner, T. *Angew. Chem., Int. Ed.* **2002**, *41*, 48−76.
(6) Jeffrey, G. A.; Saenger, W. *Hydrogen Bonding in Biological Structures*; Springer-Verlag: New York, 1991.
(7) Trumpower, B. L., Ed. *Functions of Quinones in Energy Conserving Systems;* Academic Press: New York, 1982.
(8) Lenaz, G., Ed. *Coenzyme Q. Biochemistry, Bioenergetics and Clinical Applications of Ubiquinone;* John Wiley & Sons: Chichester, U.K., 1985.
(9) Cramer, W. A.; Knaff, D. B. In *Energy Transduction in Biological Membranes. A Textbook of Bioenergetics*; Springer-Verlag: New York, 1990; pp 193−238.
(10) Blankenship, R. E. *Molecular Mechanisms of Photosynthesis*; Blackwell Science: Cambridge, MA, 2001.
(11) Klinman, J. P.; Mu, D. *Annu. Rev. Biochem.* **1994**, *63*, 299−344.
(12) Weil, J. A.; Bolton, J. R.; Wertz, J. E. *Electron Paramagnetic Resonance, Elementary Theory and Practical Applications*; Wiley: New York, 1994.
(13) Schweiger, A.; Jeschke, G. *Principles of Pulse Electron Paramagnetic Resonance*; Oxford University Press: Oxford, U.K., 2001.

10.1021/ja0392014 CCC: $27.50

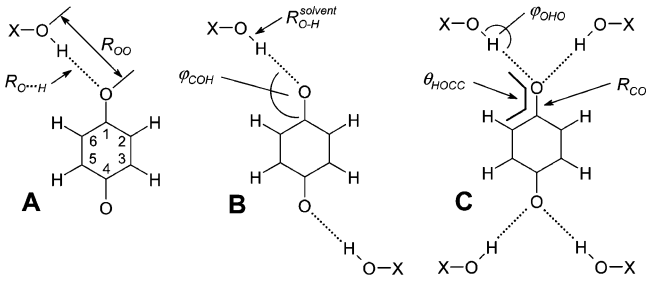

Figure 1. Structure and numbering of the *p*-benzosemiquinone radical anion. Three small model systems have been used in the calculations: $BQ^{\bullet-}$ in coordination with one (A), two (B), or four (C) solvent molecules X-OH (X = H or alkyl). The hydrogen bond geometries are discussed by bond lengths *R*, bond angles φ, and dihedral angles θ. Additionally, a model system with 20 water molecules was used; see Figure 3.

$I \geq 1$, the quadrupole interaction probes the electric field gradient at the nucleus, which is described by the nuclear quadrupole coupling tensor χ_i. All these parameters are sensitive to the local environment of the radical and therefore implicitly contain information on the hydrogen-bonding characteristics. Consequently, models were developed for obtaining hydrogen-bond lengths and geometries from such magnetic resonance data. For example, the point-dipole model can be used for a correlation between the magnitude of the anisotropic HFCC of the bridging hydrogen and the hydrogen-bond length.[13−17] Furthermore, the empirical fits of Soda and Chiba[18,19] and Hunt and MacKay[20,21] allow the estimation of hydrogen-bond lengths from ^{2}H NQCC, when ^{2}H is substituted for ^{1}H in the respective hydrogen bond. However, there are only a few examples for the determination of ^{2}H NQCC of paramagnetic systems with biological relevance.[22−29]

In this work, we will focus on the *p*-benzosemiquinone radical anion ($BQ^{\bullet-}$) as a simple quinone model in coordination with water and different alcohols (Figure 1). This model is attractive for a theoretical study because it is moderate in size and many experimental data are available. Our data will be discussed in comparison with the results of the recent EPR and ^{1}H/^{2}H ENDOR investigation at 35 GHz on the benzosemiquinone radical anion of Flores et al.[28] Proton hyperfine tensors,[16,17] as well as ^{13}C and ^{17}O HFCC[30−35] and **g**-tensor values,[36,37] are also available from other studies.

Theoretical investigations can be helpful for the interpretation of the experimental data by providing reasonable guess parameters that are required in the simulations of complex experimental spectra. In consequence, not only geometries but also spectroscopic data of $BQ^{\bullet-}$ were already the subject of several theoretical investigations. Chipman[38] and O'Malley and coworkers[39−40] employed density functional theory (DFT) methods for the calculation of hyperfine coupling constants of $BQ^{\bullet-}$, and *g*-factors of $BQ^{\bullet-}$ were computed in the past by semiempirical methods[41,42] and Hartree−Fock linear response theory.[43] More recently, DFT-based **g**-tensor studies have been reported.[44,45] To our knowledge, calculations of NQCC (e.g., of ^{2}H in hydrogen bonds) have not been published yet for $BQ^{\bullet-}$ or any other quinone radical.

The aim of this work is the calculation of a consistent set of EPR parameters (HFCC, NQCC, and **g**-tensors) for geometry-optimized structures of $BQ^{\bullet-}$ in coordination with different solvent molecules. The same density functional and basis sets are used in the calculation of all EPR parameters. This "integrated" approach makes the simultaneous comparison between theory and experiment for three different physical properties possible, which is very valuable for an appraisal of the theoretical results. The results of such an approach can also be used in more complex systems to deduce the exact geometry of the radical and its surrounding—including the hydrogen-bond situation—from a comparison of experiment and theory.

This study is divided into the following parts: First, various model systems including a different number of water ligands were studied in view of an appropriate description of the radical anion−solvent interactions (see Figure 1). The calculated EPR parameters were used for a simulation of ENDOR spectra. Pulse Q-band ^{2}H ENDOR investigations were performed on $BQ^{\bullet-}$ in D_2O to supplement the continuous-wave (CW) ENDOR results from the previous study by Flores et al.[28] In a subsequent step, the water molecules were replaced by alcohol molecules to investigate their influence on the EPR parameters. Finally, the H-bond length dependence of the **g**-tensor, the HFCC, and the NQCC was studied by varying the hydrogen-bond distances. Thereby, the quality of the point-dipole approximation for the estimation of H-bond lengths from anisotropic HFCC of bridging hydrogens[17] and the accuracy of empirical fits for the estimation of H-bond lengths from NQCC of bridging ^{2}H nuclei[18−21] were tested.

(14) O'Malley, P. J.; Chandrashekar, T. K.; Babcock, G. T. In *Antennas and Reaction Centers of Photosynthetic Bacteria. Structure, Interactions, and Dynamics*; Michel-Beyerle, M. E., Ed.; Springer-Verlag: Berlin, 1985; pp 339−344.
(15) Feher, G.; Isaacson, R. A.; Okamura, M. Y.; Lubitz, W. In *Antennas and Reaction Centers of Photosynthetic Bacteria. Structure, Interactions, and Dynamics*; Michel-Beyerle, M. E., Ed.; Springer-Verlag: Berlin, 1985; pp 174−189.
(16) O'Malley, P. J.; Babcock, G. T. *J. Am. Chem. Soc.* **1986**, *108*, 3995−4001.
(17) MacMillan, F.; Lendzian, F.; Lubitz, W. *Magn. Reson. Chem.* **1995**, *33*, S81−S93.
(18) Soda, G.; Chiba, T. *J. Chem. Phys.* **1969**, *50*, 439−455.
(19) Soda, G.; Chiba, T. *J. Phys. Soc. Jpn.* **1969**, *26*, 249−261.
(20) Hunt, M. J.; MacKay, A. L. *J. Magn. Reson.* **1974**, *15*, 402−414.
(21) Hunt, M. J.; MacKay, A. L. *J. Magn. Reson.* **1976**, *22*, 295−301.
(22) Force, D. A.; Randall, D. W.; Britt, R. D.; Tang, X. S.; Diner, B. A. *J. Am. Chem. Soc.* **1995**, *117*, 12643−12644.
(23) Bennati, M.; Stubbe, J.; Griffin, R. G. *Appl. Magn. Reson.* **2001**, *21*, 389−410.
(24) van Dam, P. J.; Willems, J. P.; Schmidt, P. P.; Pötsch, S.; Barra, A. L.; Hagen, W. R.; Hoffman, B. M.; Andersson, K. K.; Gräslund, A. *J. Am. Chem. Soc.* **1998**, *120*, 5080−5085.
(25) Doan, P. E.; Fan, C. L.; Hoffman, B. M. *J. Am. Chem. Soc.* **1994**, *116*, 1033−1041.
(26) Fan, C. L.; Kennedy, M. C.; Beinert, H.; Hoffman, B. M. *J. Am. Chem. Soc.* **1992**, *114*, 374−375.
(27) Flores, M.; Abresch, E.; Lubitz, W.; Isaacson, R.; Feher, G. *Biophys. J.* **2002**, *82*, 2334.
(28) Flores, M.; Isaacson, R. A.; Calvo, R.; Feher, G.; Lubitz, W. *Chem. Phys.* **2003**, *294*, 401−413.
(29) Lubitz, W.; Isaacson, R.; Flores, M.; Sinnecker, S.; Lendzian, F.; Feher, G. *Biophys. J.* **2002**, *82*, 2333.
(30) Gulick, W. M.; Geske, D. H. *J. Am. Chem. Soc.* **1966**, *88*, 4119−4124.
(31) Burghaus, O. Ph.D. Thesis, Freie Universität Berlin, Germany, 1991.
(32) Stone, E. W.; Maki, A. H. *J. Am. Chem. Soc.* **1965**, *87*, 454−458.
(33) Das, M. R.; Venkataraman, B. *J. Chem. Phys.* **1961**, *35*, 2262−2263.
(34) Das, M. R.; Fraenkel, G. K. *J. Chem. Phys.* **1965**, *42*, 1350−1360.
(35) Strauss, H. L.; Fraenkel, G. K. *J. Chem. Phys.* **1961**, *35*, 1738−1750.
(36) Hales, B. J. *J. Am. Chem. Soc.* **1975**, *97*, 5993−5997.
(37) Burghaus, O.; Plato, M.; Rohrer, M.; Möbius, K.; MacMillan, F.; Lubitz, W. *J. Phys. Chem.* **1993**, *97*, 7639−7647.
(38) Chipman, D. M. *J. Phys. Chem. A* **2000**, *104*, 11816−11821.
(39) O'Malley, P. J. *J. Phys. Chem. A* **1997**, *101*, 6334−6338.
(40) O'Malley, P. J.; Collins, S. J. *Chem. Phys. Lett.* **1996**, *259*, 296−300.
(41) Knüpling, M.; Törring, J. T.; Un, S. *Chem. Phys.* **1997**, *219*, 291−304.
(42) Törring, J. T.; Un, S.; Knüpling, M.; Plato, M.; Möbius, K. *J. Chem. Phys.* **1997**, *107*, 3905−3913.
(43) Engström, M.; Vahtras, O.; Ågren, H. *Chem. Phys.* **1999**, *243*, 263−271.
(44) Kaupp, M.; Remenyi, C.; Vaara, J.; Malkina, O. L.; Malkin, V. G. *J. Am. Chem. Soc.* **2002**, *124*, 2709−2722.
(45) Neyman, K. M.; Ganyushin, D. I.; Rinkevicius, Z.; Rösch, N. *Int. J. Quantum Chem.* **2002**, *90*, 1404−1413.

2. Methods and Materials

2.1. Computational Details. The *p*-benzosemiquinone radical anion $BQ^{\bullet-}$ was coordinated with water, methanol, ethanol, isopropyl alcohol (2-propanol), or *tert*-butyl alcohol (1,1-dimethylethanol) molecules. All calculations were performed employing the popular density functional[46−48] hybrid method B3LYP.[49−51] This functional has proven to provide excellent electronic structures and spectroscopic parameters of quinone radical ions.[52] Constrained and complete geometry optimizations were carried out employing the double-ζ Dunning−Huzinaga basis set.[53,54] Polarization and diffuse functions from the same authors were used for all elements, including hydrogen. The EPR-II basis set has been employed for the calculation of all magnetic and electric properties at the optimized geometries.[55] This basis set was generated from the Dunning−Huzinaga functions by uncontracting the Gaussian functions in the outer core−inner valence region with a subsequent reoptimization of the contraction coefficients. The EPR-II basis set was designed to yield accurate hyperfine splittings, i.e., close to the basis set limit, while still being moderate in size.[55] We expect a similar quality of the calculated NQCC employing the EPR-II basis set. Double-ζ basis sets are also known to be sufficiently accurate for **g**-tensor calculations on quinone radical anions.[44] Optimizations were carried out employing the Gaussian 98 software,[56] and all electric and magnetic properties have been calculated by the electronic structure system ORCA.[57] ^{1}H/^{2}H isotope effects are not covered by our approach but are expected to be small in this system.[28]

EPR *g*-values g_i with $i = x, y, z$ were calculated employing the coupled-perturbed Kohn Sham equations[58] in conjunction with the effective, parametrized one-electron spin−orbit operator of Koseki et al.[59−61] Spin−orbit coupling, spin-polarization, relativistic mass, and diamagnetic gauge correction are covered by this approach, which allows also the use of hybrid density functionals and the treatment of open shell systems other than doublet states. A similar approach was recently developed by Kaupp and co-workers.[62]

The hyperfine interaction A_i with $i = x, y, z$ consists of an isotropic (Fermi contact) part A_{iso} and an anisotropic (dipole−dipole) contribution A_i': $A_i = A_i' + A_{iso}$. In the special case of $A_x' = A_y' \neq A_z'$, axial symmetry is obtained, while rhombic symmetry follows for the case with three different eigenvalues. First-order isotropic HFCC A_{iso} and anisotropic HFCC A_i' were calculated without further approximations as expectation values by use of the B3LYP spin density matrix and the appropriate atomic integrals over Gaussian basis functions.[63]

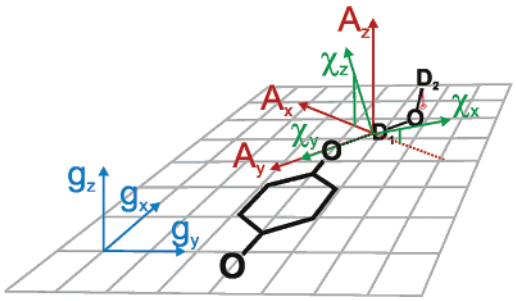

Figure 2. Orientation of the **g**-tensor and the bridging deuterium hyperfine (***A***) and nuclear quadrupole tensors (χ) in the molecular frame of the BQ radical anion coordinated with one D_2O. Note that the **g**-tensor axes are collinear with the molecular axes *x*, *y*, and *z* of BQ (with symmetric H-bonds). $\vec{g}_x$, $\vec{g}_y$, $\vec{A}_x$, $\vec{A}_y$, and $\vec{\chi}_y$ are expected to lie in the quinone plane to a good approximation. $\vec{\chi}_z$ and $\vec{\chi}_x$ are expected to be parallel and perpendicular to the plane of the water (D_2O) molecule.

Nuclear quadrupole coupling constants $\chi_i = e^2q_iQ/h$ were obtained from electric field gradients q_i employing the ^{2}H nuclear quadrupole moment *Q* of 28.75×10^{-24} m^2.[64] The constant 675.5 ($=e^2Q/4\pi h\epsilon_0 a_0^3$) was used for the conversion from *q* (au) to χ (kilohertz), which is marginally larger than the value of 672, given by Huber.[65] Both parameters give rise to NQCC differing by less than 2 kHz, which is negligible in relation to the intrinsic computational and experimental errors. The asymmetry parameter η of the nuclear quadrupole tensor is given as $\eta = |(\chi_2 - \chi_1)/\chi_3|$, with $|\chi_1| < |\chi_2| < |\chi_3|$.

Tensor orientations are calculated in this work without restrictions; the coordinate systems are given in Figure 2. For an idealized system one can expect the following tensor orientations: the **g**-tensor has two components (labeled as g_x and g_y) in the plane of the quinone, and the larger one points along the C−O bonds (labeled as g_x).[37] The main component of the hyperfine tensor of a bridging hydrogen (A_y) is directed in good approximation along the respective H-bond, while A_x and A_z should be found in the quinone plane and perpendicularly to it, respectively.[17,37] The eigenvector of the largest nuclear quadrupole tensor component χ_y is also expected to be oriented along the H-bond in first approximation, while χ_x and χ_z are oriented perpendicular and parallel to the plane of the coordinating water molecule, respectively.[66]

2.2. Experimental Details. Pulse Q-band experiments (with the Mims ENDOR sequence $\pi/2-\tau-\pi/2-$RF$-\pi/2-\tau-$echo[13]) were carried out on a Bruker ELEXSYS E580-Q spectrometer with a Super Q-FT microwave bridge. The solid-state microwave amplifier in this bridge produces a power of 0.5 W at the resonator. This is sufficient for a $\pi/2$ pulse of 30 ns in our slightly overcoupled home-built Q-band CW-ENDOR resonator. The design of this resonator is similar to that described previously.[67] The RF π-pulse for proton ENDOR ($\nu_H = 52$ MHz at g_e) in this resonator is ~15 μs with a 300 W ENI amplifier (type 3200L). The ENDOR efficiency for ^{2}H ($\nu^2_H \approx 8$ MHz) is substantially lower and an optimum RF pulse of 50 μs length was used for the Mims ENDOR experiments. To facilitate comparison with the CW ENDOR experiments by Flores et al.,[28] the absorption mode (Mims) ENDOR spectra were "pseudomodulated" with a modulation amplitude of 70 kHz by use of the Bruker Xepr software. To increase

(46) Hohenberg, P.; Kohn, W. *Phys. Rev. B* **1964**, *136*, 864.
(47) Kohn, W.; Sham, L. J. *Phys. Rev.* **1965**, *140*, 1133.
(48) Koch, W.; Holthausen, M. C. *A Chemist's Guide to Density Functional Theory*; Wiley−VCH: Weinheim, Germany, 2000.
(49) Lee, C. T.; Yang, W. T.; Parr, R. G. *Phys. Rev. B* **1988**, *37*, 785−789.
(50) Becke, A. D. *J. Chem. Phys.* **1993**, *98*, 5648−5652.
(51) Stephens, P. J.; Devlin, F. J.; Chabalowski, C. F.; Frisch, M. J. *J. Phys. Chem.* **1994**, *98*, 11623−11627.
(52) O'Malley, P. J. *Antioxid. Redox. Sign.* **2001**, *3*, 825−838.
(53) Dunning, T. H. *J. Chem. Phys.* **1970**, *53*, 2823−2833.
(54) Dunning, T. H.; Hay, P. J. In *Modern Theoretical Chemistry*; Schaefer, H. F., Ed.; Plenum: New York, 1976.
(55) Barone, V. In *Recent Advances in Density Functional Methods*; Chong, D. P., Ed.; World Scientific Publishing Co.: Singapore, 1996.
(56) Frisch, M. J.; Trucks, G. W.; Schlegel, H. B.; Scuseria, G. E.; Robb, M. A.; Cheeseman, J. R.; Zakrzewski, V. G.; Montgomery, J. A., Jr.; Stratmann, R. E.; Burant, J. C.; Dapprich, S.; Millam, J. M.; Daniels, A. D.; Kudin, K. N, Strain, M. C.; Farkas, O.; Tomasi, J.; Barone, V.; Cossi, M.; Cammi, R.; Mennucci, B.; Pomelli, C.; Adamo, C.; Clifford, S.; Ochterski, J.; Petersson, G. A.; Ayala, P. Y.; Cui, Q.; Morokuma, K.; Malick, D. K.; Rabuck, A. D.; Raghavachari, K.; Foresman, J. B.; Cioslowski, J.; Ortiz, J. V.; Stefanov, B. B.; Liu, G.; Liashenko, A.; Piskorz, P.; Komaromi, I.; Gomperts, R.; Martin, R. L.; Fox, D. J.; Keith, T.; Al-Laham, M. A.; Peng, C. Y.; Nanayakkara, A.; Gonzales, C.; Challacombe, M.; Gill, P. M. W.; Johnson, B.; Chen, W.; Wong, M. W.; Andres, J. L.; Gonzales, C.; Head-Gordon, M.; Reploge, E. S.; Pople, J. A. *Gaussian 98*, revision A.7, A.9; Gaussian, Inc.: Pittsburgh, PA, 1998.
(57) Neese, F. ORCA, an ab initio, Density Functional and Semiempirical Program Package, Version 2.2; Max-Planck-Institut für Bioanorganische Chemie: Mülheim an der Ruhr, Germany, 2001.
(58) Neese, F. *J. Chem. Phys.* **2001**, *115*, 11080−11096.
(59) Koseki, S.; Schmidt, M. W.; Gordon, M. S. *J. Phys. Chem.* **1992**, *96*, 10768−10772.
(60) Koseki, S.; Gordon, M. S.; Schmidt, M. W.; Matsunaga, N. *J. Phys. Chem.* **1995**, *99*, 12764−12772.
(61) Koseki, S.; Schmidt, M. W.; Gordon, M. S. *J. Phys. Chem. A* **1998**, *102*, 10430−10435.
(62) Malkina, O. L.; Vaara, J.; Schimmelpfennig, B.; Munzarová, M.; Malkin, V. G.; Kaupp, M. *J. Am. Chem. Soc.* **2000**, *122*, 9206−9218.
(63) Neese, F.; Solomon, E. I. In *Magnetism: Molecules to Materials*; Miller, J. S., Drillon, M., Eds.; Wiley−VCH: Weinheim, Germany, 2003; pp 345−466.
(64) Weil, J. A.; Rao, P. S. *Bruker EPR/ENDOR Frequency Table*; Bruker: Karlsruhe, Germany, 1998.
(65) Huber, H. *J. Chem. Phys.* **1985**, *83*, 4591−4598.
(66) Chiba, T. *J. Chem. Phys.* **1964**, *41*, 1352−1358.
(67) Sienkiewicz, A.; Smith, B. G.; Veselov, A.; Scholes, C. P. *Rev. Sci. Instrum.* **1996**, *67*, 2134−2138.

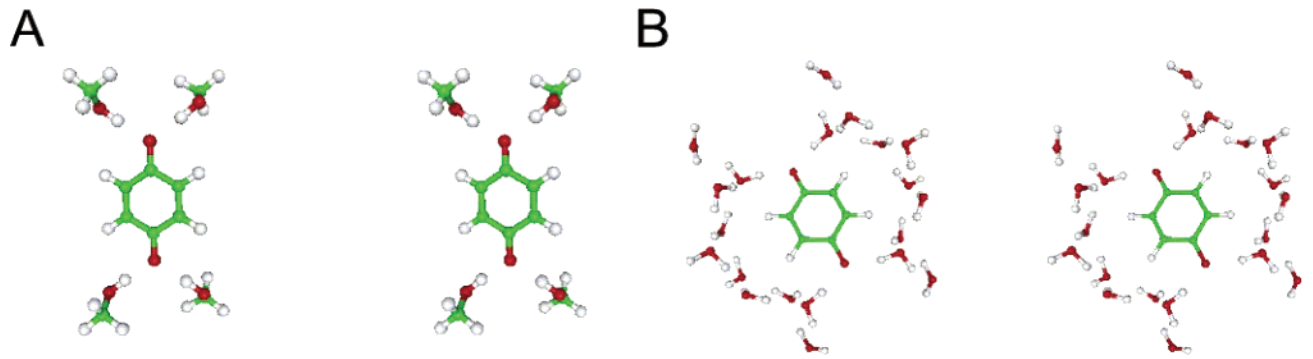

Figure 3. Stereoviews of the benzosemiquinone radical anion in coordination with four methanol molecules (A) and 20 water molecules (B). In all calculations, in-plane hydrogen bonding was found. In model B, the quinone is directly hydrogen-bonded to four water molecules (first solvent shell), which are in turn hydrogen-bonded to three further solvent molecules (second solvent shell), respectively. Some additional water molecules from the third solvent shell were used for completing the model system.

Table 1. Geometrical H-Bond Parameters for Benzosemiquinone Radical Anion−Solvent Complexes[a]

	number of solvent molecules											
	one				two				four			
	$R_{O\cdots H}$	φ_{COH}	φ_{OHO}	θ_{HOCC}	$R_{O\cdots H}$	φ_{COH}	φ_{OHO}	θ_{HOCC}	$R_{O\cdots H}$	φ_{COH}	φ_{OHO}	θ_{HOCC}
water[b]	1.70	127	171	2.5	1.72	127	171	2.5	1.76	127	171	1.1
methanol	1.68	128	171	1.2	1.70	126	173	1.0	1.75	124	174	1.1
ethanol	1.67	127	173	0.7	1.69	127	174	1.6	1.75	124	175	1.3
2-propanol	1.69	129	171	2.7	1.71	128	172	1.3	1.76	124	175	2.1
tert-butanol	1.71	130	171	0.8	1.73	129	171	1.0	1.78	122	180	6.6

[a] H-bond lengths R are given in angstroms; angles φ and θ are given in degrees (see Figure 1). [b] Values of $R_{O\cdots H} = 1.74$ Å, $\varphi_{COH} = 112°$, $\varphi_{OHO} = 165°$, and $\theta_{HOCC} = 7.2°$ were obtained for the $BQ^{\bullet-}$/20-water system.

the orientation selectivity of the ENDOR experiment, the microwave pulse durations were extended to 44 ns ($\pi/2$). Between the first two microwave pulses, the spacing τ was 300 ns. ENDOR data were recorded at $T = 80$ K. The spectra were accumulated in 500 points (10 echoes/point) over 200−600 scans depending on field positions with a repetition time of 4 ms.

ENDOR spectral simulations and fittings were carried out by a dedicated Matlab procedure based on the analytical expressions for $I = 1$ nuclear transition frequencies developed by Muha.[68] To speed up the simulations, an ENDOR intensity of unity was assumed. It should be noted that the ENDOR effect for small hyperfine couplings is reduced due to the τ-dependent blind spot effect in the Mims ENDOR spectra.[13] These effects were, however, not taken into account in the simulations.

1,4-Benzoquinone (BQ) was obtained from Aldrich and purified by vacuum sublimation. The respective radical anion was produced as described[28] by dissolving BQ in D_2O in a quartz tube (o.d. = 3 mm/i.d. = 2 mm, $c = 1 \times 10^{-3}$ mol/L), which was deoxygenated by argon bubbling. To the deoxygenated solution was added 0.1 M benzyltrimethylammonium hydroxide as base, together with a trace of benzoin, which serves as a reductant. The sample was rapidly frozen in liquid nitrogen.

3. Results and Discussion

3.1. H-Bond Geometries. A comparison of the calculated optimal hydrogen-bond lengths $R_{O\cdots H}$ of the model systems with one or two solvent molecules shows similar, short values ranging from 1.67 to 1.73 Å for all employed solvent types (Table 1). Somewhat increased hydrogen-bond lengths of $R_{O\cdots H} = 1.75-1.78$ Å were obtained for the model systems with four solvent molecules (water or alcohols), while an intermediate value of 1.74 Å was obtained for the model system with 20 water molecules (Figure 3). The largest $R_{O\cdots H}$ values can be reported for the complexes with the bulkier $BQ^{\bullet-}$/*tert*-butyl alcohol complexes, but there is no simple correlation between $R_{O\cdots H}$ and the size of the solvent molecules.

The obtained hydrogen bonds lie in the plane of the quinone to a very good approximation. The calculated dihedral angles θ_{HOCC} (see Figure 1) are in all cases smaller than 8°. A noticeable decrease of the H-bond energy for $BQ^{\bullet-}$/1 water was reported to occur for dihedral angles θ_{HOCC} larger than 10°.[44] The non-H-bonded hydrogen nuclei of the water molecules or the respective alkyl chains of the alcohols X (see Figure 1) are twisted out of the quinone π-plane in all calculations (Figure 2).

All the systems displayed in Figure 1 are characterized by almost linear H-bonds (φ_{OHO} close to 180°) and form angles close to 120° with the sp^2-hybridized carbonyl oxygen atoms.[5] The calculated H-bond lengths $R_{O\cdots H}$ and angles φ_{COH} are in good agreement with the DFT results on the $BQ^{\bullet-}$/4 water system, obtained by O'Malley ($R_{O\cdots H} = 1.78-1.79$ Å and $\varphi_{COH} = 121-124°$).[39]

3.2. EPR Parameters of $BQ^{\bullet-}$ in Coordination with Water Molecules in Optimized Geometries. By use of model systems with one, two, four, and 20 water molecules, the influence of different solvent models on the EPR parameters was investigated (Table 2).

g-Tensors. Considering the model system with four water molecules, the orientation of the calculated **g**-tensor is in very good agreement with the molecular axes system of the quinone (see Figure 2). In contrast, a slight rotation around g_z ($\leq 5°$) in the direction of the hydrogen bonds was found for $BQ^{\bullet-}$ in coordination with only one or two H-donor molecules. In general, g-values $g_x > g_y > g_z$ with g_z close to g_e were calculated for all model systems, in line with experimental findings.[28,36,37]

A more detailed comparison of our results with the experimental values shows that especially the large g_x component is somewhat overestimated in our calculations. Its computed value depends strongly on the number of coordinated water molecules; the agreement between theory and experiment is improved when proceeding from one water molecule to two, four, and 20 water molecules. The remaining deviation between theory and experiment can be attributed to systematic errors introduced by present-day density functionals.[44] This allows the use of scaling factors,[69] which were, however, not applied in our work. Very

(68) Muha, G. M. *J. Magn. Reson.* **1982**, *49*, 431−443.

(69) Kaupp, M. *Biochemistry* **2002**, *41*, 2895−2900.

Table 2. Calculated H-Bond Lengths[a] and Spectroscopic Parameters[b] of $BQ^{\bullet-}$ in Coordination with One, Two, Four, and 20 Water (D_2O) Molecules: Comparison with Experimental Results

	number of water molecules				
	one	two	four	20	exptl[c]
$R_{O\cdots H}$	1.70	1.72	1.76	1.74	
g_x	2.0090	2.0083	2.0075	2.0069	2.0065
g_y	2.0058	2.0057	2.0055	2.0055	2.0053
g_z	2.0022	2.0022	2.0022	2.0022	2.0023
g_{iso}	2.0057	2.0054	2.0051	2.0049	2.0047
A'_x (^{2}H)	−0.51	−0.52	−0.48	−0.46	−0.47
A'_y (^{2}H)	+1.07	+1.09	+0.99	+0.99	+0.95
A'_z (^{2}H)	−0.56	−0.57	−0.51	−0.53	−0.49
A_{iso} (^{2}H)	+0.01	+0.01	+0.03	−0.02	+0.03
χ_x (^{2}H)	−0.122	−0.125	−0.134	−0.122	−0.134
χ_y (^{2}H)	+0.205	+0.211	+0.229	+0.209	+0.208
χ_z (^{2}H)	−0.083	−0.086	−0.095	−0.087	−0.074
η	0.19	0.18	0.17	0.17	0.29

[a] H-bond lengths are given in angstroms. [b] *g*-values, isotropic (A_{iso}) and anisotropic (A'_i) HFCC as well as NQCC (χ_i) of the bridging deuterium nuclei (megahertz) and the nuclear quadrupole asymmetry parameter $\eta = |(\chi_x - \chi_z)/\chi_y|$. Idealized tensor orientations are given in Figure 2. For Euler angles, see Supporting Information. [c] Experimental results are from Flores et al.[28] Similar parameters (megahertz) of $A'_x = -0.45$, $A'_y = +0.92$, $A'_z = -0.46$, $A_{iso} = +0.03$, $\chi_x = -0.124$, $\chi_y = +0.208$, $\chi_z = -0.084$, and $\eta = 0.19$ were obtained in this work employing Q-band Mims ENDOR.

good agreement between theory and experiment was recently also obtained by Kaupp et al.,[44] employing a perturbational sum-over-states DFT approach ($BQ^{\bullet-}$ in coordination with four 2-propanol molecules; $g_x = 2.00671$, $g_y = 2.00517$, and $g_z = 2.00227$).

In contrast to our work, only a small **g**-tensor dependence on the number of incorporated solvent molecules was found in an UHF-PM3 study employing Rayleigh−Schrödinger perturbation theory,[41] but other DFT-based **g**-tensor calculations gave also noticeable differences in the *g*-values obtained for isolated $BQ^{\bullet-}$ and the radical anion in coordination with four solvent molecules.[44,45] This strong **g**-tensor dependence on the surroundings is already known, e.g., for duroquinone,[37] ubiquinone,[70] and phylloquinone[71] radicals. In these systems, a lowering of the g_x and g_y values was observed by exchanging aprotic nonpolar for protic polar solvents.[37,70,71] For tyrosyl radicals in ribonucleotide reductases, distinctly lower *g*-values were also found for the hydrogen-bonded species.[24,72]

^{2}H Hyperfine Coupling Constants of the Bridging Deuteriums. The anisotropic hyperfine tensors of the bridging deuterium nuclei in $BQ^{\bullet-}/D_2O$ are close to axial symmetry with a large positive eigenvalue A'_y of about 1 MHz (see Table 2). Its orientation is almost collinear with the H-bond direction with deviations of less than 10°. A second component A'_x is also found to lie in the quinone plane. In consequence, the HFCC tensor axes system differs from the **g**-tensor orientation only by a rotation around g_z (see Figure 2). Values between −30° and −50° have been calculated for this Euler angle; −30° would be expected for an ideal hydrogen bond with $\varphi_{COH} = 120°$. The isotropic part of the electron spin−nuclear spin coupling between the radical and the bridging deuterium is smaller than 0.03 MHz in all cases, showing that the interaction is almost purely dipolar. A comparison of the computed ^{2}H hyperfine tensor with the experimental results shows good agreement, especially for the model systems with four and 20 water molecules.

^{2}H Nuclear Quadrupole Coupling Constants of the Bridging Deuteriums. In general, the calculated nuclear quadrupole tensors are rather small and deviate from axial symmetry. The main principal value $e^2qQ/h \equiv \chi_y$ is positive and is close to 0.2 MHz for all model systems. The corresponding vector is oriented approximately along the respective hydrogen-bond direction, yielding Euler angles from −46° to −50° for the rotation around *z* with respect to the *g*-frame (see Figure 2). The directions of the other two nuclear quadrupole tensor components of the bridging deuterium nuclei depend on the orientation of the respective water molecule. The geometry optimizations yielded structures with the second (not hydrogen-bonded) H or D atom of the water(s) twisted out of the quinone plane. In consequence, and contrary to the **g**- and **A**-tensor orientations, the smallest tensor component $\vec{\chi}_z$ is parallel to the normal of the water plane, whereas g_z and A_z of the bridging hydrogen (deuterium) atoms are found perpendicular to the quinone π-plane (see Figure 2). The calculated orientation of $\vec{\chi}_z$ and the obtained order $|\chi_y| > |\chi_x| > |\chi_z|$ are in line with results from deuterium magnetic resonance spectroscopy investigations on single crystals containing O−D···O bonds.[66] Thus, a complete characterization of the nuclear quadrupole tensor provides the opportunity to draw conclusions on the orientation of the H-donor molecules with respect to the quinone radical. This is of particular interest for biological systems such as proteins with unusual H-bond geometries.

Upon comparison of the calculated and measured ^{2}H NQCC, best agreement of the major component is obtained for the model system with 20 water molecules (see Table 2).

Choice of the Model System. It is likely that a radical anion dissolved in a protic solvent interacts with a large number of solvent molecules. Therefore, a model including more than one solvent shell is more appropriate than the smaller systems with only one, two, or four water molecules. This consideration is encouraged by the small deviations between theory and experiment achieved for the $BQ^{\bullet-}$/20 water system (see Table 2). Calculations on such large systems are, however, still somewhat demanding with respect to computational resources. Therefore it was interesting to find out whether the experimental conditions are already well described by model systems including only one solvent shell. $BQ^{\bullet-}$ in coordination with a single water molecule is not likely to be an appropriate model system for symmetry reasons. Upon comparison of the model systems with two and four water molecules, a small preference for the model system with four solvent molecules was found. A higher coordination of the carbonyl oxygen atoms is also feasible for simple electrostatic reasons as demonstrated by electrostatic potential plots.[52]

Computation of ENDOR Spectra and Direct Comparison with Experimental Results. The calculation of the **g**-tensors and the complete hyperfine and quadrupole tensors of the bridging deuterium nuclei makes a simulation of orientation-selected ENDOR spectra possible.

Figure 4A shows the experimental Q-band Mims ENDOR spectra obtained at field values corresponding to g_x, g_y, and g_z both in absorption mode and in pseudomodulated form. The latter representation was chosen in order to facilitate comparison

(70) Nimz, O.; Lendzian, F.; Boullais, C.; Lubitz, W. *Appl. Magn. Reson.* **1998**, *14*, 255−274.
(71) Teutloff, C.; Hofbauer, W.; Zech, S. G.; Stein, M.; Bittl, R.; Lubitz, W. *Appl. Magn. Reson.* **2001**, *21*, 363−379.
(72) Schmidt, P. P.; Andersson, K. K.; Barra, A. L.; Thelander, L.; Gräslund, A. *J. Biol. Chem.* **1996**, *271*, 23615−23618.

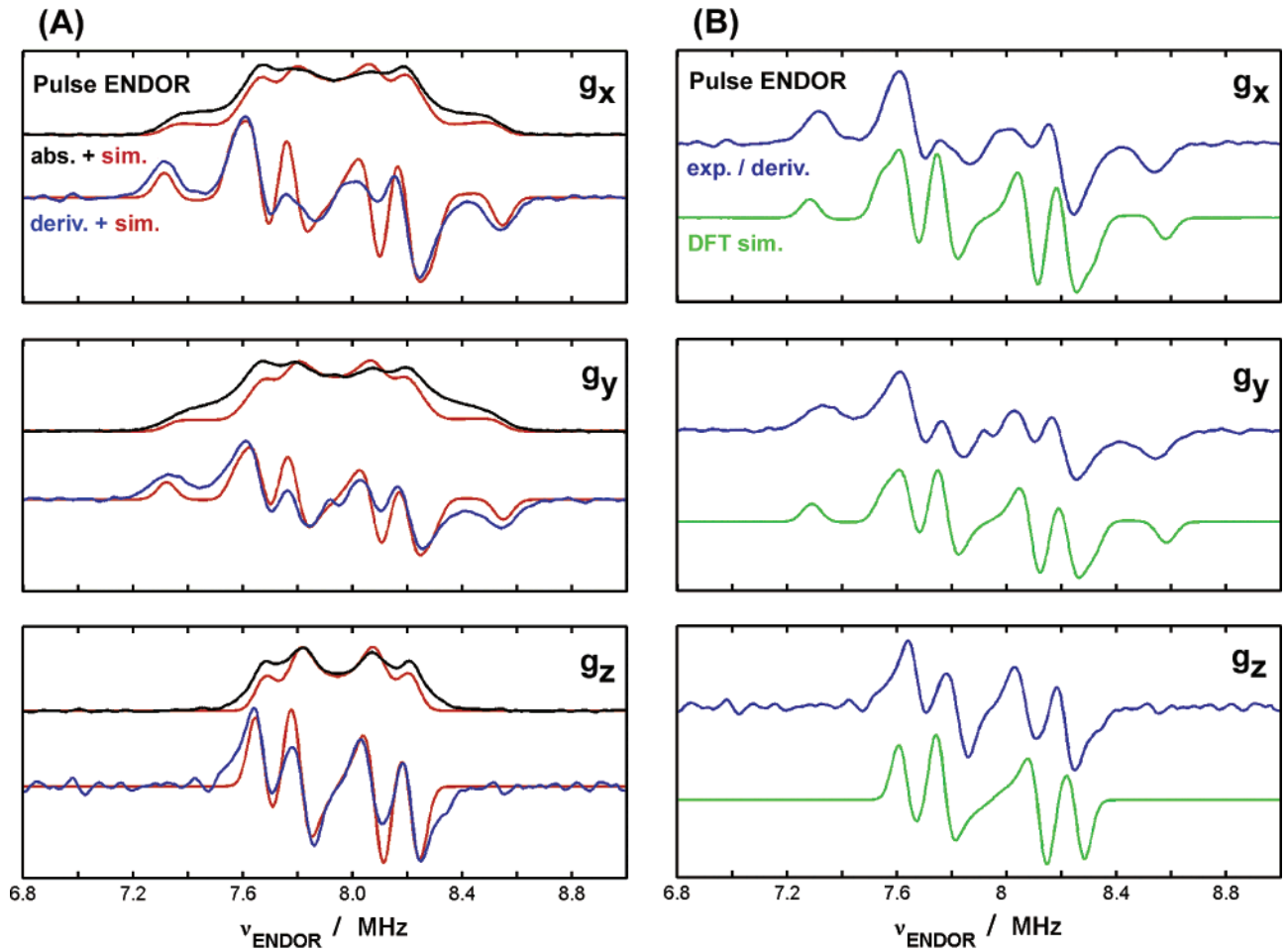

Figure 4. (A) Q-band (34.088 GHz) pulse ^{2}H ENDOR (Mims) absorption spectra (black lines) of $BQ^{\bullet-}-h_4$ in D_2O at $T = 80$ K recorded at the three principal **g**-tensor values in the EPR spectrum. The simulated spectra (red lines) were generated from parameters that were fitted on the pseudomodulated spectra (blue lines): hyperfine couplings (−0.42, 0.95, −0.43) MHz with Euler angles (−36, 4, 0)° and nuclear quadrupole couplings (−0.124, 0.208, −0.084) MHz with Euler angles (−20, 28, 0)°. The ENDOR line widths are 80, 80, and 70 kHz for the g_x, g_y, and g_z positions, respectively. The simulations have been optimized on the positions of the spectral features in the pseudomodulated Mims ENDOR spectra. It should be noted that the central "blind spot" characteristic for Mims ENDOR causes the intensities in the center of the experimental spectra to be reduced as compared with the simulations.[13] (B) Calculated ^{2}H ENDOR spectra (first derivative) for $BQ^{\bullet-}$ in coordination with 20 water (D_2O) molecules (green lines) in comparison with the experimental orientation-selected pseudomodulated pulse ENDOR (Mims) spectra at 34 GHz (blue). The DFT results (eigenvalues of the hyperfine, nuclear quadrupole, and **g**-tensors and the corresponding Euler angles) have been used without any fitting in the ENDOR simulations; only the line width parameters (not available from the theoretical work) were adjusted. For further experimental details see text.

with previous CW ENDOR studies.[28] The correspondence between the two ENDOR techniques turned out to be very good (see Supporting Information). Note that in the pulse ENDOR studies the inner lines (close to the nuclear Larmor frequency) appear weak and somewhat distorted. This is due to the τ-dependent ENDOR efficiency characteristic of Mims-ENDOR[13] (not taken into account in the simulations). In Figure 4B a comparison is made between the pseudomodulated Mims ENDOR and simulated ENDOR spectra. For the simulations the theoretical tensor values from the DFT calculations of the BQ radical anion in coordination with 20 water molecules (Table 2) were used without further fitting or adjustment. This direct comparison underlines the high quality of the calculated data and shows the potential of the theoretical method to predict experimental spectra.

3.3. EPR Parameters of $BQ^{\bullet-}$ in Coordination with Alcohol Molecules. In this section, calculations of the EPR parameters for $BQ^{\bullet-}$ in coordination with four water and with four methanol, ethanol, 2-propanol, or *tert*-butyl alcohol molecules are presented. All these systems are characterized by only slightly different H-bond lengths lying between 1.75 and 1.78 Å (Table 1). No influence of the solvent type on the **g**-tensor was found: Similar *g*-values within four decimal places are obtained for all solvents, provided that the same number of H-bonds is formed. Furthermore, very similar ^{1}H, ^{13}C, and ^{17}O hyperfine and ^{2}H nuclear quadrupole data are calculated for the different solvents. The obtained values are compared with experimental and other theoretical results[39] in Table 3. In addition to the hyperfine data of the bridging hydrogens, the almost axially symmetric hyperfine tensors of the quinone ring hydrogens (see Figure 1) and of the neighboring carbon atoms are also well described by our work in comparison to the experiments.[17,37] Somewhat larger deviations occur for the ^{13}C and ^{17}O hyperfine coupling constants of the carbonyl groups, which are very sensitive to the surrounding and thus to hydrogen bonding.

A comparison of the calculated H-bond lengths (Table 1) and EPR parameters (Table 3) obtained for the different solvents indicates that sterical hindrance obviously plays no important role for these systems. This result is fully supported by the

Table 3. Calculated EPR Parameters (B3LYP/EPR-II//B3LYP/DZPD) for $BQ^{\bullet-}$, Coordinated by Four Solvent Molecules (Figure 1)[a]

	water	methanol	ethanol	2-propanol	*tert*-butanol	exptl	other DFT results[b]
Bridging Hydrogens[c]							
A'_x (^{1}H)	−3.15	−3.17	−3.17	−3.13	−3.07	−3.00	−3.0
A'_y (^{1}H)	+6.47	+6.42	+6.43	+6.33	+6.18	+6.02	+6.1
A'_z (^{1}H)	−3.32	−3.26	−3.26	−3.20	−3.11	−3.01	−3.0
A_{iso} (^{1}H)	+0.19	+0.18	+0.16	+0.17	+0.13	+0.34	+0.1
χ_x (^{2}H)	−0.134	−0.132	−0.131	−0.133	−0.134	−0.134	
χ_y (^{2}H)	+0.229	+0.226	+0.225	+0.227	+0.228	+0.208	
χ_z (^{2}H)	−0.095	−0.093	−0.093	−0.094	−0.095	−0.074	
Quinone Hydrogens[d]							
A_1' (^{1}H)	−3.36	−3.36	−3.36	−3.36	−3.36	−3.26	−3.5
A_2' (^{1}H)	−2.49	−2.51	−2.51	−2.51	−2.51	−2.05	−2.4
A_3' (^{1}H)	+5.85	+5.87	+5.87	+5.87	+5.87	+5.32	+5.9
A_{iso} (^{1}H)	−6.39	−6.36	−6.36	−6.34	−6.33	−6.62	−6.4
Carbonyl Oxygens[e] (^{17}O)							
A_1'	−75.4	−74.3	−74.2	−73.9	−73.6	−69.5	−78.7
A_2'	+37.3	+36.8	+36.7	+36.6	+36.5	+30.5	+39.0
A_3'	+38.1	+37.5	+37.4	+37.3	+37.1	+38.9	+39.8
A_{iso}	−21.4	−21.0	−21.0	−20.9	−20.7	−22.1	−22.0
Carbonyl Carbons (^{13}C)							
A_1'	−12.24	−12.62	−12.68	−12.75	−12.81		−13.0
A_2'	−9.21	−9.67	−9.73	−9.82	−9.90		−9.7
A_3'	+21.45	+22.29	+22.41	+22.57	+22.71		+22.8
A_{iso}	−4.28	−3.64	−3.56	−3.46	−3.33	−0.7[f]	−3.8
Other Ring Carbons (^{13}C)							
A_1'	−6.46	−6.41	−6.41	−6.39	−6.35		−6.9
A_2'	−6.03	−5.97	−5.97	−5.95	−5.91		−6.5
A_3'	+12.50	+12.38	+12.37	+12.33	+12.26		−13.3
A_{iso}	−1.69	−1.82	−1.83	−1.88	−1.90	−1.66[g]	−1.6

[a] ^{2}H nuclear quadrupole coupling constants χ, and ^{1}H, ^{13}C, and ^{17}O isotropic and anisotropic hyperfine coupling constants A_{iso} and A'. All values are given in megahertz. [b] Theoretical results: B3LYP/EPR-III//B3LYP/EPR-III, considering $BQ^{\bullet-}$/4 water.[39] [c] Experimental values are from studies performed in water (H_2O and D_2O, respectively).[28] [d] Experimental values are from studies performed in 2-propanol.[37] [e] Experimental values are from studies performed in 2-propanol.[31] [f] Experimental value is from studies performed in water.[32] [g] Experimental value is from studies performed in ethanol/water.[34,35]

almost identical experimental ^{2}H ENDOR spectra of $BQ^{\bullet-}$, taken in D_2O, methanol-d_1, ethanol-d_1, and 2-propanol-d_1, which show very similar hyperfine and quadrupole couplings for the bridging ^{2}H nuclei in all cases (cf. Figure 5 from Flores et al.)[28]

3.4. Constrained Geometry Optimizations: Variation of Hydrogen-Bond Lengths. In the next step, surface scans for $BQ^{\bullet-}$ in coordination with one, two, and four water molecules were performed, with all hydrogen bond lengths fixed to the same value, ranging from 1.4 to 2.3 Å, in steps of 0.05 Å. After reoptimization of the molecular structures, the EPR parameters were calculated.

^{2}H Nuclear Quadrupole Coupling Constants of the Bridging Deuterium Nuclei. The main component of the nuclear quadrupole coupling tensor $\chi_y \equiv e^2qQ/h$ shows a linear dependence on $R_{O\cdots D}^{-3}$ (Figure 5). Similar observations have been used in the past to develop empirical relations for the estimation of H-bond lengths (angstroms) from nuclear quadrupole coupling constants (kilohertz) of the form[18−21]

$$e^2qQ/h = a - \frac{b}{R_{O\cdots D}^3} \qquad (1)$$

The parameter a corresponds to an extrapolated ^{2}H NQCC in the isolated hydrogen donor molecule ($R_{O\cdots D} \rightarrow \infty$), while b describes the effect of the O···D bond formation on the ^{2}H NQCC. This term, in general, leads to a smaller electric field gradient at the nucleus and thus to a decrease of the NQCC.

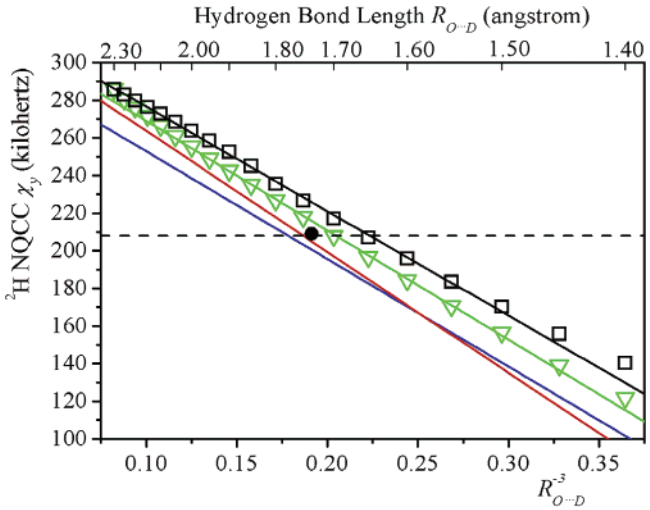

Figure 5. ^{2}H NQCC $\chi_y = e^2qQ/h$ of the bridging deuterium as a function of the hydrogen-bond length: DFT results for $BQ^{\bullet-}$ in coordination with two (green) and four (black) water molecules and comparison with the empirical fits from Soda−Chiba[18] (blue) and Hunt−MacKay[20] (red). The solid circle (●) displays the computed (single point) result for $BQ^{\bullet-}$ in coordination with 20 water molecules (complete geometry optimization, H-bond length of 1.74 Å). The black dashed line indicates the experimental value obtained for $BQ^{\bullet-}$ in D_2O.[28] Its intersection with the computed or experimental graphs gives estimates of the hydrogen-bond length, e.g., 1.78 Å from the Soda−Chiba plot.

Table 4. Linear Fit Parameters for the Estimation of Hydrogen-Bond Lengths from NQCC of the Bridging Deuterium According to Eq 1

	a (kHz)	b (kHz·Å^3)
BQ/1 water	338	474
$BQ^{\bullet-}$/1 water	331	620
$BQ^{\bullet-}$/2 water	329	596
$BQ^{\bullet-}$/4 water	336	581
Soda−Chiba[18]	310	572
Hunt−MacKay[20]	328	643

The published fit parameters a and b are given in Table 4 and are compared with the parameters obtained by least-squares fits of the computed points between 1.60 and 2.00 Å, found in our work.

Good agreement is obtained in spite of the fact that experimental results of very different molecular systems such as deuterated amino acids,[20] metal salts ($Li_2SO_4{\cdot}D_2O$ or KD_2PO_4), and carbonic acids[18] are compared with our computed results for the BQ radical anion.

In addition to the calculations on the BQ radical anion−solvent interactions, we extended our study to the neutral BQ with one water molecule. The results clearly show that there is a weaker interaction between these neutral molecules as compared to the charge−dipole interplay between $BQ^{\bullet-}$ and a solvent, which leads to larger nuclear quadrupole coupling constants (Figure 6). In the geometry-optimized structures the hydrogen-bond lengths are 1.70 Å for $BQ^{\bullet-}$/1 water and 1.95 Å for neutral BQ in coordination with one water molecule. This demonstrates that upon formation of the radical anion the H-bond gets shorter by about 0.25 Å. This is an interesting aspect for electron-transfer involving quinones in redox proteins, e.g., bacterial reaction centers.[73,74]

Due to the simple form of eq 1 it could have been assumed that the contribution of the water oxygen to the electric field gradient and the NQCC of the bridging deuterium is constant.

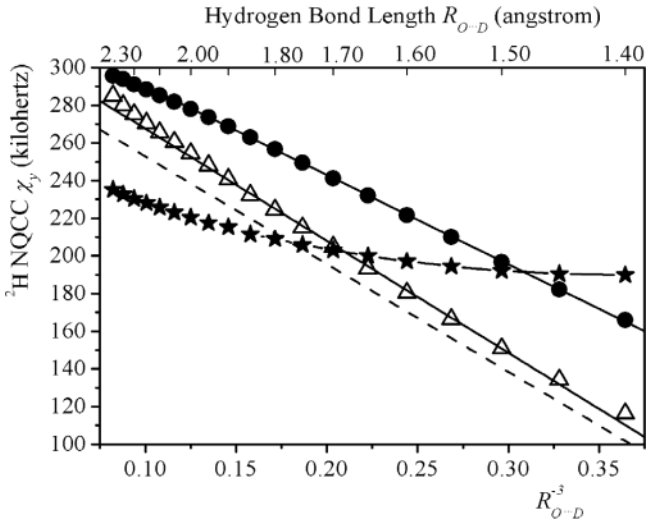

Figure 6. Nuclear quadrupole coupling constants $\chi_y = e^2qQ/h$ for $BQ^{\bullet-}$ in coordination with one water (△) compared with neutral BQ in coordination with one water (●). Also shown is the case where the O−D bond length in the water molecule is kept at a constant value of 1.0 Å, leading to an erroneous prediction of NQCC (★). For comparison, the Soda−Chiba fit is also included (---).

This is not the case, as demonstrated by an additional calculation in which the O−D bond length $R_{OD}(D_2O)$ in the water molecule was held constant with a value of 1.00 Å (Figure 6). In fact, different hydrogen-bond lengths lead to a small variation of the O−D distances within the water molecules. These small changes are already sufficient to cause major changes of the electric field gradient of the solvent oxygen, which acts on the deuterium in the hydrogen bond. Considering for example the $BQ^{\bullet-}$/4 water system, values of $R_{OD}(D_2O) = 1.037$ and 0.975 Å between the water oxygen and the H-bond forming deuterium were obtained as a consequence of hydrogen-bond formation with lengths of 1.400 and 2.300 Å, respectively. In consequence, a noticeable dependence of the fit parameters *a* and *b* on the systems can be expected. Furthermore, cases that do not show a linear dependence of the NQCC on $R^{-3}_{O\cdots D}$ cannot be excluded a priori.

Anisotropic Hyperfine Coupling Constants of the Bridging Hydrogens (^{1}H). The relation between the anisotropic hyperfine coupling constants of the bridging hydrogen (megahertz) and the H-bond length (angstroms) is given by the point-dipole model:[13]

$$A_i' = \frac{c}{R^3_{O\cdots H}}\rho_0^{\pi}(3\cos^2\Omega - 1) \qquad (2)$$

where for protons $c = g_e\beta_e g_N\beta_N/h = 79.2$ MHz·Å^3. Here, g_e and g_N are the electron and nuclear *g*-values, and β_e and β_N are the electron and nuclear Bohr magnetons. Ω is the angle between the applied field and the bond direction. The characteristic inflection points of orientation-selected ENDOR spectra correlate with values of $\Omega = 0$ for $A_y' \equiv A_{||}'$ and $\Omega = 90°$ for $A_x' = A_z' \equiv A_\perp'$ in the case of axial symmetry. The carbonyl oxygen π-spin density ρ_0^{π} plays a crucial role in this equation; we will describe it here by the calculated Löwdin p_z spin densities.[75] Although more basis-set-dependent, similar spin densities were obtained by employing the Mulliken partitioning analysis.[76] The carbonyl oxygen π-spin density depends noticeably on the hydrogen bond length (see Table 5) and is in general not known. Since ρ_0^{π} is changing with H-bond lengths, an accurate estimation of the H-bond length is difficult.

Table 5. Calculated Carbonyl−Oxygen Löwdin p_z Spin Densities ρ_0^{π} and Carbonyl Bond Lengths as a Function of the Hydrogen-Bond Lengths ($BQ^{\bullet-}$/4 Water)

$R_{O\cdots H}$ (Å)	1.400	1.500	1.600	1.700	1.763[a]	1.800	1.900	2.000	2.300	∞[b]
R_{CO} (Å)	1.297	1.294	1.291	1.288	1.286	1.285	1.282	1.281	1.279	1.275
ρ_0^{π}	0.204	0.212	0.219	0.224	0.227	0.229	0.233	0.236	0.242	0.256

[a] Value from complete geometry optimization. [b] Calculation for isolated $BQ^{\bullet-}$, i.e., without water molecules.

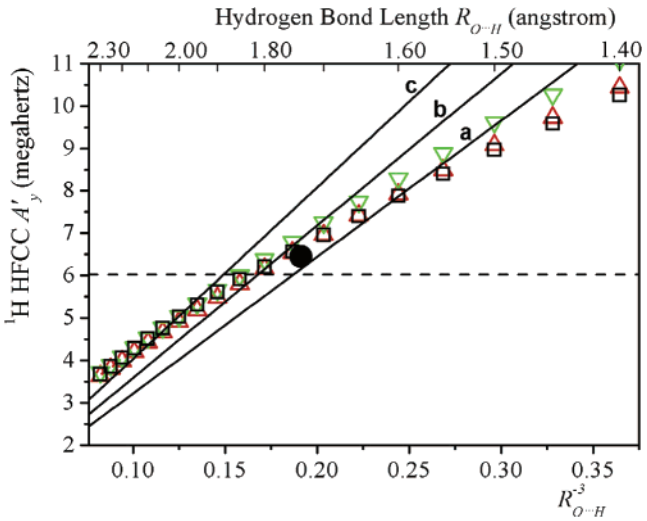

Figure 7. ^{1}H anisotropic HFCC $A_{||}' = A_y'$ of the bridging hydrogen as a function of hydrogen-bond length: DFT results for $BQ^{\bullet-}$ in coordination with one (red triangles), two (green triangles), or four water molecules (black squares) and comparison with point-dipole plots (black lines) employing carbonyl oxygen π-spin densities of (a) 0.20, (b) 0.23, and (c) 0.26; see text. The solid circle (●) displays the computed result for $BQ^{\bullet-}$ in coordination with 20 water molecules. The black dashed line indicates the experimental value obtained for $BQ^{\bullet-}$ in D_2O.[28] The H-bond length can be estimated from the intersection of this line with the point-dipole plots.

From the simple point-dipole model, an approximate $1/R^3_{O\cdots H}$ dependence of the main hf tensor component A_y' on the H-bond length is expected. This was indeed found in the DFT calculations. Figure 7 shows plots calculated by using the point-dipole approach with three different ρ_0^{π} values. In the literature it has been stated that the point-dipole model is not valid for $R_{O\cdots H} < 2.5$ Å.[13] From our work a limit of 2.0 Å can be estimated, when the calculated Löwdin oxygen π-spin density of the isolated (i.e., not hydrogen bonded) quinone radical anion with $\rho_0^{\pi} = 0.26$ for the point-dipole calculation is taken ($BQ^{\bullet-}$/4 water complex). By use of the spin density of 0.23 for the point-dipole plot, good agreement with the computed HFCC is obtained, especially around $R_{O\cdots H} \approx 1.8$ Å (see Figure 7). For the completely geometry-optimized system with $R_{O\cdots H} = 1.76$ Å, a value of $\rho_0^{\pi} = 0.227$ was obtained, in perfect agreement with the experimental estimate of 0.228, which is the ratio of the measured ^{17}O HFCC $A_z' = -65.6$ MHz and the computed ^{17}O value of −288 MHz for a spin density of unity in the p_z orbital.[17]

The point-dipole model does not work for short hydrogen-bond lengths due to the increased covalent character of the

(73) Feher, G.; Allen, J. P.; Okamura, M. Y.; Rees, D. C. *Nature* **1989**, *339*, 111−116.
(74) Lubitz, W.; Feher, G. *Appl. Magn. Reson.* **1999**, *17*, 1−48.
(75) Löwdin, P.-O. *Adv. Quantum Chem.* **1970**, *5*, 185−199.
(76) Mulliken, R. S. *J. Chem. Phys.* **1962**, *36*, 3428−3439.

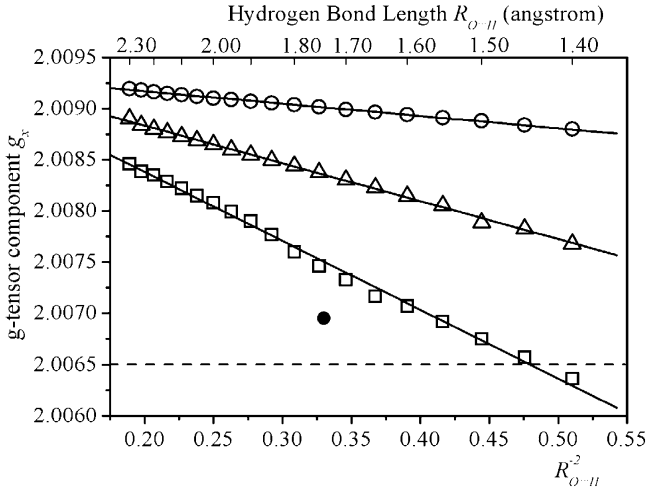

Figure 8. Major **g**-tensor component g_x as a function of the hydrogen-bond length: DFT results for $BQ^{\bullet-}$ in coordination with one (○), two (△), and four water molecules (□). The solid circle (●) displays the computed result for $BQ^{\bullet-}$ in coordination with 20 water molecules. The dashed line indicates the experimental g_x value obtained for $BQ^{\bullet-}$ in D_2O.[28]

H-bond that leads to significant overlap of the MOs of the contributing fragments and consequently to nonclassical terms that are not covered in the point-dipole approximation. Taking for example an H-bond length $R_{O\cdots H} = 1.4$ Å, an oxygen π-spin density of 0.20 was calculated, but the corresponding point-dipole function deviates obviously quite strongly from the calculated hyperfine coupling constants at 1.4 Å (see Figure 7).[77]

It is important to note that the coordination of one, two or four water molecules results in rather similar data points for the anisotropic HFCC in Figure 7. In contrast, the nuclear quadrupole coupling constants and, in particular, the **g**-tensor components depend strongly on the chosen model system, that means, on the interaction of the entire radical with solvent molecules (Figures 5 and 8). The magnitude of the anisotropic HFCC is mainly determined by the corresponding H-bond formed by the respective nucleus. Therefore, this property is quite well suited for a correlation with the hydrogen-bond length.

Isotropic HFCC. For the whole range of hydrogen-bond lengths considered, only a very small isotropic ^{1}H HFCC of the bridging hydrogen could be obtained, which increases versus shorter hydrogen-bond distances. When, for example, the case of $BQ^{\bullet-}$ in coordination with four water molecules is considered, a negative isotropic coupling constant of −0.8 MHz was obtained for hydrogen-bond lengths of 1.4 Å, a change in sign occurs between 1.60 and 1.65 Å, and at 2.3 Å a value of +0.2 MHz is obtained.

The ring hydrogens give rise to continuously increasing isotropic hyperfine coupling constants with larger hydrogen-bond distances (+6.14 MHz for 1.4 Å and +6.43 MHz for 2.3 Å). Although these values are easily accessible from the experiment, their dependence on the hydrogen-bond length is too small to draw any meaningful conclusion. Our calculations with four solvent molecules result in four equivalent quinone hydrogen nuclei (see Figure 1). If only one solvent molecule is considered, a strong asymmetry in the HFCC of the protons at positions 2 and 6 and at positions 3 and 5 can be observed due to the fact that the spin densities of the carbon atoms at positions 1, 3, and 5 are distinctly larger than those of the carbon atoms at positions 2, 4, and 6 (see Figure 1). Such an asymmetry plays no role for quinones in solution and could not be found in calculations on model systems with two or four water molecules (without use of symmetry restrictions). Nevertheless, it is important for radicals with an asymmetric coordination from a protein environment.[71,74,78,79]

g-Tensors. Knüpling et al.[41] found in their work on semiquinone radicals a $1/R^2_{O\cdots H}$ dependence of the **g**-tensor on the H-bond length. This finding is in agreement with our results, which is displayed for g_x in Figure 8. These authors proposed the application of a multipole expansion for the electrostatic potential around the radical, including monopole−monopole/monopole−dipole ($1/R^2$), dipole−dipole ($1/R^3$), and dispersion contributions ($1/R^6$). Apparently, the computed g-value dependence is already well described by truncating the expansion after the $1/R^2$ term. Only for $BQ^{\bullet-}$ in coordination with four water molecules a slight deviation from the expected straight line was found (Figure 8).[80]

In contrast to the anisotropic HFCC, g_x is very sensitive to the number of coordinated water molecules. This is not unexpected for an integral property of the radical and may be used to determine whether H-bonds are formed or not. Furthermore, one can probably also draw conclusions on the number and strengths of these bonds. It is interesting to note that the formation of a single H-bond is only of minor influence on g_x (see Figure 8). This is in accordance with EPR experiments on the phylloquinone radical anion $VK_1^{-\bullet}$ in photosystem I. Despite the existence of a rather strong hydrogen bond to one of the carbonyl oxygens,[79,81] g-values close to those of isolated $VK_1^{-\bullet}$ in apolar, nonprotic solvents (ethers) were measured.[71] The model system with two water molecules leads to distinctly lowered g_x values in our calculations. This result is in agreement with the reduced g-anisotropy obtained for the ubiquinones of bacterial reaction centers, liganded by two (different) hydrogen donor molecules.[74,82] The smallest g-shifts were calculated for the model system with 20 water molecules. These data are best to compare with in vitro experiments performed in polar protic solvents.

3.5. Estimation of Hydrogen-Bond Lengths from the Computed Magnetic Resonance Parameters. The point-dipole model and the Soda−Chiba or Hunt−MacKay fits allow the estimation of H-bond lengths from HFCC and NQCC. We applied these relations to our computed EPR and ENDOR data to test their quality; the estimated H-bond lengths are compared with our results from geometry optimization in Table 6. For completeness, also the experimental EPR data were used for an estimation of the H-bond lengths.[28]

(77) Despite the rather satisfactory performance of the simple point-dipole approximation in the present case, it should be noted that the estimation of spin densities at a given nucleus from the population on the associated atom is of limited reliability. The spin population samples the whole region of space where the orbitals of the spin-carrying atom have nonzero amplitudes while the physical spin density samples a single point in space; see Neese, F. *J. Phys. Chem. A* **2001**, *105*, 4290−4299.

(78) Grimaldi, S.; Ostermann, T.; Weiden, N.; Mogi, T.; Miyoshi, H.; Ludwig, B.; Michel, H.; Prisner, T. F.; MacMillan, F. *Biochemistry* **2003**, *42*, 5632−5639.
(79) Teutloff, C.; Bittl, R.; Lubitz, W. *Appl. Magn. Reson.* **2004**, in press.
(80) This effect can be traced back to a formation of H-bonds between the coordinating water molecules. It is only observed for large H-bond distances to the quinone in the model with four water molecules. The effect cannot appear in the calculations on the model systems with one or two water molecules (coordinated to different carbonyl oxygens of the quinone radical anion), where an almost perfect linear fitting was found.
(81) Jordan, P.; Fromme, P.; Witt, H. T.; Klukas, O.; Saenger, W.; Krauss, N. *Nature* **2001**, *411*, 909−917.
(82) Isaacson, R. A.; Lendzian, F.; Abresch, E. C.; Lubitz, W.; Feher, G. *Biophys. J.* **1995**, *69*, 311−322.

Table 6. Estimation of Hydrogen Bond Lengths from Anisotropic ^{1}H HFCC and ^{2}H NQCC of the Bridging Hydrogen Atoms

	EPR/ENDOR parameters (MHz)		estimated hydrogen bond length (Å) from			
	A'_y	χ_y	anisotropic HFCC[a]	NQCC[b]	NQCC[c]	DFT geometry optimization
calcd for 2 waters	+7.10	+0.211	1.72	1.79	1.76	1.72
calcd for 4 waters	+6.47	+0.229	1.78	1.92	1.87	1.76
calcd for 20 waters	+6.45	+0.209	1.78	1.78	1.75	1.74
exptl[28]	+6.02	+0.208	1.82	1.78	1.75	

[a] Point-dipole model; an oxygen π spin density of $\rho_0^\pi = 0.23$ was used. [b] According to ref 18 (see Table 4). [c] According to ref 20 (see Table 4).

Anisotropic Hyperfine Coupling Constants. By application of eq 2 to the calculated anisotropic HFCC of the bridging hydrogen atoms obtained for the model systems with two, four, and 20 water molecules, hydrogen-bond lengths between 1.72 and 1.78 Å were estimated. These results are in good agreement with the H-bond lengths obtained from geometry optimization (1.72−1.76 Å). This underlines the validity of the point-dipole model for H-bonds distinctly shorter than 2 Å in the case of $BQ^{\bullet-}$, but it is obvious from Figure 7 that an appropriate value of the carbonyl oxygen π-spin density must be available. From the experimental ^{1}H HFCC of 6.02 ± 0.12 MHz, a hydrogen-bond length of 1.82 ± 0.01 Å is obtained with the point-dipole model.[28] The performed ^{2}H ENDOR experiments suffer from a reduced sensitivity in comparison to the ^{1}H ENDOR studies due to the smaller magnetic moment of deuterium. Nevertheless, similar H-bond lengths of 1.81 and 1.83 Å were obtained from the experimental ^{2}H anisotropic hyperfine coupling constants of +0.95 MHz (CW ENDOR)[28] and +0.92 MHz (pulse ENDOR, this work), respectively.

Nuclear Quadrupole Coupling Constants. The estimated H-bond lengths from eq 1 are also displayed in Table 6, employing the Soda−Chiba and Hunt−MacKay fits. A comparison with the H-bond lengths from geometry optimization shows good agreement for the model systems with two and 20 water molecules, while too-long H-bonds are predicted for the model system with four water molecules. The fit parameters from our DFT calculations (Table 4) lead to an underestimation of H-bond lengths in the analysis of experimental data. The reason is an overestimation of the experimental NQCC by about 10% ($BQ^{\bullet-}$/4 water) or, probable, an underestimation of the H-bond length by about 0.05 Å ($BQ^{\bullet-}$/2 water). A general overestimation of NQCC within the applied level of theory is, however, unlikely, since a test calculation for the free water molecule gave a NQCC of 315 kHz, which is in excellent agreement with the experimental values of 310,[83] 314,[84] and 319 kHz[85] given in the literature.

The estimation of hydrogen-bond lengths from nuclear quadrupole coupling constants is a very attractive approach since no other parameters than the ^{2}H NQCC are required (e.g., like the oxygen π-spin density for the point-dipole model). A challenge is, however, to obtain the NQCC from the experiments with sufficient accuracy.

4. Summary and Conclusions

In this work, benzosemiquinone radical anion−solvent interactions have been investigated by studying $BQ^{\bullet-}$ in coordination with one, two, four, and 20 solvent molecules. Best agreement between theory and experiment was in general found for the largest model system with 20 water molecules. A simulation of orientation-selected pulse and CW ENDOR spectra at *Q*-band frequencies employing the calculated spectroscopic parameters of $BQ^{\bullet-}$ with a large solvent shell (20 waters) gave very good agreement with the experimental ENDOR spectra. This allows the conclusion that the calculated geometry of the system is fairly close to reality. The oxygens of $BQ^{\bullet-}$ each form two hydrogen bonds ($R_{O\cdots H} = 1.74$ Å) with water molecules of the first solvation shell. These H-bonds are almost linear (deviation ≤ 15°) and lie in the π-plane of the $BQ^{\bullet-}$ radical to good approximation (deviation ≤ 7°). The water molecules are twisted out of the quinone plane. In a second solvent shell further H-bonds are formed to the oxygen atoms of the water molecules in the first shell. The third solvation shell shows a similar picture. It is important to note that the second shell has a nonnegligible effect on the geometry and electronic structure of the molecules in the first solvation shell.

The coordination of the *p*-benzosemiquinone radical anion with water, methanol, ethanol, 2-propanol, or *tert*-butyl alcohol molecules revealed that all these systems are characterized by similar hydrogen-bond lengths and geometries to the radical. Consequently, also similar EPR parameters were calculated for all these complexes, in full agreement with the experimental findings. Sterical hindrance, therefore, does not play an important role in these systems. However, for the alcoholic solvent shell a maximum of only four solvent molecules has been considered so far.

In another set of calculations, the hydrogen-bond lengths $R_{O\cdots H}$ were varied between 1.4 and 2.3 Å in model systems with one, two and four water molecules. Here, the well-known $1/R^3_{O\cdots H}$ dependence of the NQCC of a bridging deuterium[18,20] could be confirmed. It was shown that the change of the ^{2}H NQCC is mainly resulting from small changes of the O−D bond length in the water molecule. The hydrogen-bond length can be estimated from the ^{2}H NQCC without knowledge of additional parameters of the system. Furthermore, the orientation of the water molecule hydrogen-bonded to the radical anion can be determined from the quadrupole tensor. There are, however, some limitations caused by the difficulties in accurately measuring the complete ^{2}H nuclear quadrupole coupling tensors of paramagnetic systems by ^{2}H ENDOR or electron spin echo envelope modulation (ESEEM) methods.

For not too short H-bond distances, a $1/R^3_{O\cdots H}$ dependence was also found for the purely dipolar HFCC of the bridging hydrogen. Here, the point-dipole model is well suited for a fairly accurate estimation of H-bond lengths from dipolar ^{1}H HFCC. It is applicable for hydrogen-bond lengths down to ≈1.7 Å. However, the spin density of the carbonyl oxygen must be known, which is only available from independent EPR experiments on ^{17}O-labeled compounds. For an estimate, calculated values can be used.

It could further be shown that the **g**-tensor shows a $1/R^2_{O\cdots H}$ dependence on the H-bond length. However, the strong dependence of the *g*-shifts on the detailed structure and polarity of the surroundings of the radicals makes it very difficult if not impossible to derive a general relationship between the *g*-shift and the H-bond length that could be used in practice.

Hydrogen bonding to quinone acceptors is widely found in proteins; examples are the quinones acting as electron acceptors

(83) Bluyssen, H.; Verhoeve, J.; Dymanus, A. *Phys. Lett. A* **1967**, *A 25*, 214.
(84) Treacy, E. B.; Beers, Y. *J. Chem. Phys.* **1962**, *36*, 1473.
(85) Thaddeus, P.; Loubser, J. H. N.; Krisher, L. C. *J. Chem. Phys.* **1964**, *40*, 257.

in reaction centers of photosynthetic bacteria and green plants and algae.[10] Particularly well studied are the ubiquinones Q_A and Q_B in the reaction centers of *Rhodobacter sphaeroides*, for which extensive magnetic resonance and other spectroscopic data already exist.[74,86,87] The different physical properties of these cofactors have been interpreted as resulting from the specific properties of the binding sites of the proteins, in which hydrogen bonding plays a dominant role. It is believed that the effects are of general importance for many similar quinones in other redox proteins (see, e.g., refs 71, 78, 79, and 88−92). DFT calculations based on the available X-ray crystallographic structures of these protein-bound quinones and quinone radical anions are currently under way in our laboratory.

Acknowledgment. This work is dedicated to Professor Dr. George Feher on the occasion of his 80th birthday. We thank Ch. Laurich and G. Klihm (MPI Mülheim) for technical assistance and F. Lendzian (TU Berlin) and R. Isaacson (UCSD) for their help with the design and construction of the Q-band ENDOR resonator used in the experiments. M. Flores and G. Feher (UCSD) are gratefully acknowledged for helpful discussions. This work has been supported by the Max Planck Society and the Konrad-Zuse-Zentrum Berlin, which generously provided computational resources. Development of algorithms for spin Hamiltonian parameter predictions are supported by a DFG grant to F.N. within the priority program "Molecular Magnetism". Support by Fonds der Chemischen Industrie (F.N., W.L.) is also gratefully acknowledged.

Supporting Information Available: Energies and EPR parameters of different $BQ^{\bullet-}$/4 H_2O conformers (influence of symmetry); Euler angles of the hyperfine and nuclear quadrupole tensors of the bridging deuterium nuclei for all investigated $BQ^{\bullet-}$/water systems; Cartesian coordinates (angstroms) for $BQ^{\bullet-}$ in coordination with water and alcohols; and comparison of the pulse ^2H ENDOR (Mims) experiments in this study with previously recorded CW ENDOR spectra from Flores et al.[28] (print, PDF). This information is available free of charge via the Internet at http://pubs.acs.org.

JA0392014

(86) Feher, G. *Appl. Magn. Reson.* **1998**, *15*, 23−38.
(87) Feher, G.; Okamura, M. Y. *Appl. Magn. Reson.* **1999**, *16*, 63−100.
(88) Deligiannakis, Y.; Hanley, J.; Rutherford, A. W. *J. Am. Chem. Soc.* **1999**, *121*, 7653−7664.
(89) Muhiuddin, I. P.; Rigby, S. E. J.; Evans, M. C. W.; Amesz, J.; Heathcote, P. *Biochemistry* **1999**, *38*, 7159−7167.
(90) MacMillan, F.; Lendzian, F.; Renger, G.; Lubitz, W. *Biochemistry* **1995**, *34*, 8144−8156.
(91) Rigby, S. E. J.; Evans, M. C. W.; Heathcote, P. *Biochim. Biophys. Acta* **2001**, *1507*, 247−259.
(92) Rigby, S. E. J.; Evans, M. C. W.; Heathcote, P. *Biochemistry* **1996**, *35*, 6651−6656.